



Nonmodal energetics of electromagnetic drift waves

Suzana J. Camargo, Michael K. Tippet, and Iberê L. Caldas

Citation: [Physics of Plasmas \(1994-present\)](#) **7**, 2849 (2000); doi: 10.1063/1.874134

View online: <http://dx.doi.org/10.1063/1.874134>

View Table of Contents: <http://scitation.aip.org/content/aip/journal/pop/7/7?ver=pdfcov>

Published by the [AIP Publishing](#)



Re-register for Table of Content Alerts

Create a profile.



Sign up today!



Nonmodal energetics of electromagnetic drift waves

Suzana J. Camargo^{a),b)}

Universidade Estadual Paulista, Av. Dr. Ariberto Pereira da Cunha, 333, 12500-000, Guaratinguetá, SP, Brazil

Michael K. Tippett^{a),c)}

Centro de Previsão do Tempo e Estudos Climáticos, Instituto Nacional de Pesquisas Espaciais, Rodovia Presidente Dutra km 40, 12630-000, Cachoeira Paulista, SP, Brazil

Iberê L. Caldas^{d)}

Instituto de Física, Universidade de São Paulo, CP: 66318, 05315-970, São Paulo, SP, Brazil

(Received 17 January 2000; accepted 23 February 2000)

The linear properties of an electromagnetic drift-wave model are examined. The linear system is non-normal in that its eigenvectors are not orthogonal with respect to the energy inner product. The non-normality of the linear evolution operator can lead to enhanced finite-time growth rates compared to modal growth rates. Previous work with an electrostatic drift-wave model found that nonmodal behavior is important in the hydrodynamic limit. Here, similar behavior is seen in the hydrodynamic regime even with the addition of magnetic fluctuations. However, unlike the results for the electrostatic drift-wave model, nonmodal behavior is also important in the adiabatic regime with moderate to strong magnetic fluctuations. © 2000 American Institute of Physics.

[S1070-664X(00)02707-5]

I. INTRODUCTION

The observed transport of particles and energy at the plasma edge in magnetic confinement devices, e.g., tokamaks, is much larger than predicted by neoclassical transport theory.¹ Experimental evidence relates this anomalous transport to observed density, electric potential, and magnetic field fluctuations.² Drift waves with amplitudes and wave numbers comparable to those of observed fluctuations result from plasma density and temperature gradients.³ Drift waves produce anomalous particle and energy diffusion along these spatial gradients. There is also experimental evidence of waves with drift-wave characteristics in the central region of the tokamak.⁴ Drift-wave turbulence is therefore assumed to be one of the mechanisms responsible for anomalous transport in tokamaks, especially at the plasma edge.

Another place where drift waves may play a role is in the transition from poor confinement (L) to improved confinement regimes (H) in tokamaks. Although extensive experimental and theoretical studies of the L – H transition have been performed, it is still not completely understood.^{5–7} Experimental evidence suggests that core plasma instabilities related to ion temperature gradient modes change into drift-type mode near the plasma edge.⁸ It has also been suggested that the edge turbulence could have its origin in the plasma center, where the magnetic fluctuations have a fundamental role.⁹ These facts suggest that the coupling between electrostatic turbulence and Alfvén waves are significant¹⁰ and vari-

ous models have been developed to study drift-Alfvén turbulence.^{10–13} Various numerical studies of drift-wave turbulence have been performed. One of the standard steps of the analysis is to study the linear properties of the models. Features of the nonlinear numerical simulation that cannot be accounted for by the linear analysis are attributed to nonlinear effects.¹⁴

Eigenmode analysis or normal mode analysis is a standard method of studying instabilities in fluids and plasmas and has been applied with success to many problems. However, there are notable cases in fluid dynamics where normal mode analysis fails to agree with observed instabilities.¹⁵ These failures have been attributed to the linearization of the problem. However, it has been long known that *non-normal* linear systems are potentially capable of behavior different than that suggested by their normal model analysis. A non-normal linear system is one that does not have a complete set of orthogonal eigenvectors. Recent studies have shown that some non-normal linear systems do indeed present behavior different than that suggested by their normal mode analysis. For instance, perturbations in modally stable systems can be amplified by factors of thousands as a result of non-normality.^{15,16}

The possible enhanced growth due to non-normality suggests *almost linear* mechanisms for the transition to turbulence.¹⁷ However, the general applicability of this mechanism for shear flows has been criticized¹⁸ and an alternative mechanism for obtaining subcritical turbulence has been proposed.¹⁹ Recently,²⁰ this mechanism has been examined in the Hasegawa–Wakatani equations, an electrostatic drift-wave model,²¹ and compared to nonlinear drift-wave mechanisms.²²

In this paper, we study the nonmodal linear properties of an electromagnetic extension of the Hasegawa–Wakatani

^{a)}Present address: International Research Institute for Climate Prediction, Lamont–Doherty Earth Observatory of Columbia University, P. O. Box 1000, 61 Route 9W, Palisades, NY 10964-8000.

^{b)}Electronic mail: suzana@iri.ideo.columbia.edu

^{c)}Electronic mail: tippett@iri.ideo.columbia.edu

^{d)}Electronic mail: ibere@if.usp.br

system; some aspects of this work are also discussed in Refs. 23 and 24. The role of the magnetic fluctuations in a simple nonlinear drift-wave model (without magnetic shear)^{25,26} has already been studied numerically.¹⁴ There, the results of the nonlinear numerical simulations were compared to the modal linear stability properties in order to understand the role of the nonlinear terms. However, the linear behavior of electromagnetic drift waves is not completely described by its modal growth properties in some regimes. The system presents a strong nonmodal behavior in the hydrodynamic regime for a wide range of magnetic fluctuations strengths, extending previous electrostatic drift-wave model results.²⁷ Previous electrostatic drift-wave model results showed little nonmodal behavior in the adiabatic regime. Here, we demonstrate that the adiabatic regime including moderate to strong magnetic fluctuations produces nonmodal growth with larger growth rates and different wave number than those given by normal model analysis. This regime of adiabatic electrons and moderate magnetic fluctuations is typical of tokamaks.

The organization of the paper is as follows. In Sec. II the nonlinear electromagnetic drift-wave model and the associated fluctuations energy inner product is described. The spectrum and pseudospectrum of the linear model is presented in Sec. III, demonstrating the non-normality of the system. Modal and nonmodal growth rates are compared in Sec. IV. Finally, a summary and conclusions are given in Sec. V.

II. NONLINEAR ELECTROMAGNETIC DRIFT-WAVE EQUATIONS

The electromagnetic drift-wave equations consisting of three nonlinear coupled bidimensional equations, for potential $\Phi(x,y)$, density $n_1(x,y)$, and magnetic $\Psi(x,y)$ fluctuations, are an extension of the Hasegawa–Wakatani system in slab geometry to include the magnetic fluctuations. This model was first derived in Refs. 25 and 26, and an equivalent form can be found in Ref. 28. It can also be interpreted as a restriction of tearing-mode models^{29,30} to a homogeneous magnetic geometry.

The electron density n is given by $n = n_0(1 + n_1/n_0)$, with $n_1 \ll 1$, where the equilibrium density $n_0(x)$ has a constant gradient in the negative x direction with equilibrium density scale $L_n = n_0/|dn_0/dx|$. The electrons are isothermal and the ions are cold ($T_i \ll T_e = T$); temperature gradients or fluctuations are neglected. The total magnetic field \mathbf{B} has a uniform component in the z direction, B_0 , with magnetic fluctuations in the (x,y) plane, such that $\mathbf{B} = B_0 \hat{e}_z - \nabla \times \Psi \hat{e}_z$.

The drift-wave dispersion scale $\rho_s = c\sqrt{M_i T}/eB$ and the sound speed $c_s = \sqrt{T/M_i}$ are used to define the usual drift parameter $\delta_0 = \rho_s/L_n$; M_i and M_e are the ion and electron masses, respectively. A parallel length scale L_s is also used, which is equivalent to the shear length in tearing-mode models. The fluctuations are then scaled according to $\phi = (e\Phi/T)\delta_0^{-1}$, $n = (n_1/n_0)\delta_0^{-1}$, $\psi = (\Psi/B_0\rho_s)(L_s/L_n)\delta_0^{-1}$, and $J = (J_{\parallel}/nec_s)(L_n/L_s)\delta_0^{-1}$. The adimensional variables are defined as $x \rightarrow x/\rho_s$, $y \rightarrow y/\rho_s$, $z \rightarrow z/L_s$, and $t \rightarrow tc_s/L_n$.

The electromagnetic drift-wave equations are¹⁴

$$\begin{aligned} \frac{d_E}{dt} \Omega &= \nabla_{\parallel} J, \\ \frac{d_E}{dt} n &= -\frac{\partial \phi}{\partial y} + \nabla_{\parallel} J, \\ \frac{\partial \psi}{\partial t} &= -\frac{\partial \psi}{\partial y} + \nabla_{\parallel} (n - \phi) - \frac{1}{\mathcal{A}} J, \end{aligned} \quad (1)$$

where

$$\Omega = \nabla_{\perp}^2 \phi, \quad J = -\frac{1}{\hat{\beta}} \nabla_{\perp}^2 \psi, \quad (2)$$

$$\frac{d_E}{dt} = \frac{\partial}{\partial t} + (\hat{\mathbf{z}} \times \nabla_{\perp} \phi) \cdot \nabla_{\perp}, \quad \nabla_{\parallel} = \frac{\partial}{\partial z} - (\hat{\mathbf{z}} \times \nabla_{\perp} \psi) \cdot \nabla_{\perp}, \quad (3)$$

$$\hat{\beta} = \frac{4\pi n_0 T}{B_0^2} \frac{L_s^2}{L_n^2}, \quad \mathcal{A} = \frac{c_s/L_n}{v_e} \frac{M_i}{M_e} \frac{L_s^2}{L_n^2}. \quad (4)$$

A Fourier representation is used:

$$f(x,y,z) \leftrightarrow \sum_{\mathbf{k}} f_{\mathbf{k}} e^{i(k_x x + k_y y + iK_{\parallel} z)}, \quad (5)$$

where $\mathbf{k} = (k_x, k_y)$ and K_{\parallel} is taken to be constant.

The adiabaticity parameter \mathcal{C} used in the Hasegawa–Wakatani system^{21,31} is related to \mathcal{A} : $\mathcal{C} = K_{\parallel}^2 \mathcal{A}$. We choose $K_{\parallel} = 1$ and consider the parameter \mathcal{C} instead of \mathcal{A} . The Hasegawa–Wakatani system²¹ is the electrostatic limit of the electromagnetic drift-wave model (1) obtained by taking $\psi \rightarrow 0$ and $J = \mathcal{C}/K_{\parallel}(n - \phi)$ ¹⁴. The two-dimensional magneto-hydrodynamic (MHD) equations³² can also be obtained from Eq. (1) by taking a constant density $n_1 = 0$ and $K_{\parallel} = 0$.¹⁴ Electromagnetic drift-wave equations therefore contain the dynamics of both the Hasegawa–Wakatani and the MHD equations. By varying the two free parameters \mathcal{C} and $\hat{\beta}$, a variety of regimes can be studied. The electromagnetic effects are controlled by $\hat{\beta}$; $\hat{\beta} \ll 1$ is the electrostatic regime and $\hat{\beta} \gg 1$ is the electromagnetic regime.¹⁴ Large values of \mathcal{C} correspond to an adiabatic regime, while small values of \mathcal{C} correspond to a hydrodynamic regime.³³ In our calculations we add dissipative corrections in Eq. (1), such that $\partial/\partial t \rightarrow \partial/\partial t + \mu \nabla_{\perp}^4$.¹⁴

The total energy of the fluctuations is an invariant of the purely nonlinear electromagnetic equations and is given by

$$\begin{aligned} E &= \frac{1}{2} \int d^2x \left(\|\nabla_{\perp} \phi\|^2 + n^2 + \frac{1}{\hat{\beta}} \|\nabla_{\perp} \psi\|^2 \right) \\ &= \frac{1}{2} \sum_{\mathbf{k}} \left(k^2 \phi_{\mathbf{k}}^2 + n_{\mathbf{k}}^2 + \frac{1}{\hat{\beta}} k^2 \psi_{\mathbf{k}}^2 \right), \end{aligned} \quad (6)$$

where $k = \sqrt{k_x^2 + k_y^2}$. The total fluctuation energy can be used to define a norm and an inner product on fluctuations. In particular, for any two fluctuations $\mathbf{u} = [\phi, n, \psi]$ and $\mathbf{u}' = [\phi', n', \psi']$, the total energy inner product is defined by

$$\langle \mathbf{u}, \mathbf{u}' \rangle \equiv \frac{1}{2} \sum_{\mathbf{k}} \left(k^2 \phi_{\mathbf{k}} \overline{\phi'_{\mathbf{k}}} + n_{\mathbf{k}} \overline{n'_{\mathbf{k}}} + \frac{1}{\hat{\beta}} k^2 \psi_{\mathbf{k}} \overline{\psi'_{\mathbf{k}}} \right), \quad (7)$$

where $\overline{(\quad)}$ denotes complex conjugate; $\|\mathbf{u}\| \equiv \langle \mathbf{u}, \mathbf{u} \rangle$ is the energy of the fluctuation \mathbf{u} . Two fluctuations \mathbf{u} and \mathbf{u}' are orthogonal if $\langle \mathbf{u}, \mathbf{u}' \rangle = 0$.

III. SPECTRUM AND PSEUDOSPECTRUM OF THE LINEAR MODEL

Neglecting the nonlinear terms of the electromagnetic drift-wave equations and expanding the potential, the density and the magnetic fluctuations in a double Fourier series in the nondimensionalized slab variables x and y gives for each pair of (k_x, k_y) a linear system:

$$\frac{d}{dt} \mathbf{u}_{\mathbf{k}} = \mathbf{A}_{\mathbf{k}} \mathbf{u}_{\mathbf{k}}, \quad (8)$$

where $\mathbf{u}_{\mathbf{k}} = [\phi_{\mathbf{k}}, n_{\mathbf{k}}, \psi_{\mathbf{k}}]^T$ and

$$\mathbf{A}_{\mathbf{k}} = \begin{pmatrix} -\nu k_{\perp}^4 & 0 & -iK_z/\hat{\beta} \\ ik_y & -\nu k_{\perp}^4 & iK_z k_{\perp}^2/\hat{\beta} \\ -iK_z & iK_z & -ik_y - k_{\perp}^2/\hat{\beta}C - \nu k_{\perp}^4 \end{pmatrix}. \quad (9)$$

An eigenvalue problem,

$$(\gamma \mathbf{I} - \mathbf{A}) \mathbf{u} = 0, \quad (10)$$

is obtained from assuming an exponential time-dependence $\sim e^{\gamma t}$ for the fluctuations; \mathbf{u} is the vector of Fourier components $\mathbf{u}_{\mathbf{k}}$ and \mathbf{A} is the block-diagonal matrix with entries $\mathbf{A}_{\mathbf{k}}$. The spectrum of \mathbf{A} , denoted $\Lambda(\mathbf{A})$, consists of the values of γ for which (10) has a nontrivial solution. The normal mode growth rate γ_0 is obtained by finding the eigenvalue of \mathbf{A} with the largest real part. The dependence of the electromagnetic drift-wave normal modal growth rate γ_0 on the adiabaticity C and magnetic field strength $\hat{\beta}$ has been previously calculated.¹⁴

If the linear operator \mathbf{A} were normal, or equivalently, if \mathbf{A} had a complete set of orthogonal eigenvectors, the modal growth rate γ_0 would give strong conditions on the behavior of the total fluctuation energy $\|\mathbf{u}(t)\|$. Namely, one could conclude that for any initial condition $\mathbf{u}(0)$ with unit initial energy

$$\|\mathbf{u}(t)\| \leq e^{\gamma_0 t}, \quad \max \frac{1}{2} \frac{d}{dt} \|\mathbf{u}(0)\| \leq \gamma_0, \quad t \geq 0, \quad (11)$$

the upper limits being achieved by taking $\mathbf{u}(0)$ to be the eigenvector of \mathbf{A} whose eigenvalue has real part γ_0 . However, the electromagnetic drift-wave system does not have a complete set of orthogonal eigenvectors and for non-normal dynamics the strongest statements that generally apply are

$$\|\mathbf{u}(t)\| \leq \mathcal{D} e^{\gamma_0 t}, \quad t \geq 0, \quad \lim_{t \rightarrow \infty} \frac{1}{2} \frac{1}{t} \ln \|\mathbf{u}(t)\| = \gamma_0, \quad (12)$$

for a constant \mathcal{D} greater or equal to unity. The constant \mathcal{D} is not known from the eigenvalue analysis and the modal growth rate γ_0 only limits the long-time growth rate. There-

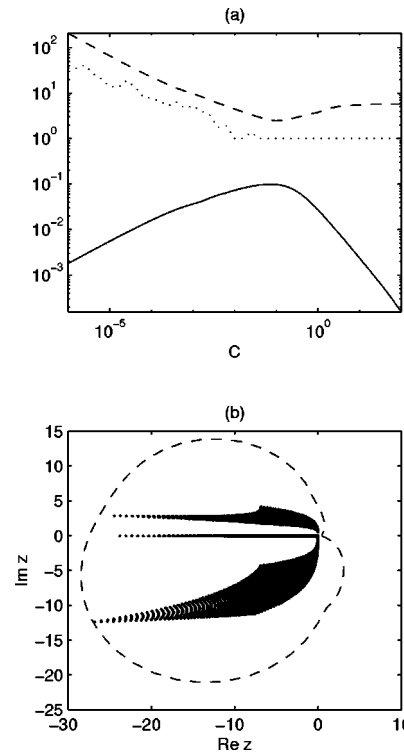


FIG. 1. (a) γ_0 (solid line), a Monte Carlo estimate of \mathcal{D}_α (dotted line), and \mathcal{D} (dashed line) as functions of the adiabaticity constant C for $\hat{\beta} = 5$. (b) The eigenvalues (circles) and the boundary of the numerical range of \mathbf{A} (dashed line) for $\hat{\beta} = 5$ and $C = 10$.

fore, the linear behavior of a non-normal system is only weakly determined by the properties of its spectrum.

Some information about the constant \mathcal{D} can be found from the *pseudospectrum* of \mathbf{A} .³⁴ A complex number z is in the ϵ pseudospectrum of \mathbf{A} , denoted $\Lambda_\epsilon(\mathbf{A})$, if z is an eigenvalue of $(\mathbf{A} + \mathbf{E})$ for $\|\mathbf{E}\| \leq \epsilon$. The ϵ -*pseudospectral abscissa* $\alpha(\epsilon)$ defined by

$$\alpha(\epsilon) = \max_{z \in \Lambda_\epsilon(\mathbf{A})} \text{Re } z, \quad (13)$$

can be used to bound \mathcal{D} from below:³⁴

$$\mathcal{D} \geq \mathcal{D}_\alpha \equiv \max_{\epsilon > 0} \frac{\alpha(\epsilon) - \alpha(0)}{\epsilon}. \quad (14)$$

Figure 1(a) shows a Monte Carlo estimate of \mathcal{D}_α and the exact value of \mathcal{D} as a function of C for $\hat{\beta} = 5$. For $C \ll 1$, \mathcal{D}_α and \mathcal{D} are considerably greater than unity, indicating the presence of enhanced nonmodal growth. Similar behavior for $C \ll 1$ was seen in an electrostatic (i.e., $\hat{\beta} \ll 1$) model.²⁷ However, in the electrostatic model considered in that work, as C increases nonmodal enhanced growth disappears and $\mathcal{D}_\alpha \approx 1$ for $C \gg 1$. Here, including moderately strong magnetic fluctuations leads to $\mathcal{D} > 1$ even for large values of the adiabaticity constant C .

Information about the rate of change of the fluctuation energy is given by the *numerical range* of \mathbf{A} , denoted $W(\mathbf{A})$

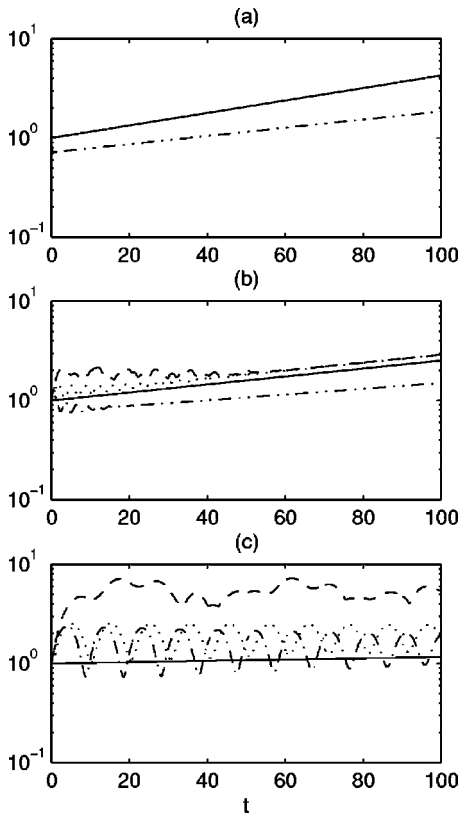


FIG. 2. The growth ratios ξ_0 (solid line), ξ_1 (dashed line), ξ_2 (dotted line), ξ_3 (dash-dot line), plotted as functions of t for $C=10$ and (a) $\hat{\beta}=10^{-3}$, (b) $\hat{\beta}=1$, and (c) $\hat{\beta}=10$.

and consisting of all complex numbers z such that for some unit vector \mathbf{u} , $z = \langle \mathbf{u}, \mathbf{A}\mathbf{u} \rangle$. Since the rate of change of the energy is given by

$$\begin{aligned} \frac{1}{2} \frac{d}{dt} \|\mathbf{u}(t)\|^2 &= \frac{1}{2} \frac{d}{dt} \langle \mathbf{u}(t), \mathbf{u}(t) \rangle \\ &= \frac{1}{2} \langle \mathbf{u}(t), \mathbf{A}\mathbf{u}(t) \rangle + \frac{1}{2} \langle \mathbf{A}\mathbf{u}(t), \mathbf{u}(t) \rangle, \end{aligned} \quad (15)$$

where $\langle \cdot, \cdot \rangle$ is the energy inner-product, the maximum rate of change of the energy is given by the *numerical abscissa* ω defined by

$$\omega = \max_{z \in W(\mathbf{A})} \text{Re } z. \quad (16)$$

If \mathbf{A} is normal, then $\omega = \gamma_0$. The eigenvalues of \mathbf{A} and the boundary of $W(\mathbf{A})$ are shown in Fig. 1(b) for $\hat{\beta}=5$ and $C=10$. The time scale suggested by the maximum modal growth rate $\gamma_0=0.0024$ is orders of magnitude different from that corresponding to the maximum rate of change of energy $\omega=3.1$. A simple calculation using Eq. (12) shows that the maximum growth rate ω can be maintained for a time no longer than 0.54.

IV. FLUCTUATION ENERGY GROWTH

Following Ref. 27, the basic quantities used to investigate the modal and nonmodal growth of electromagnetic drift waves will be the energy growth ratio $\xi(t)$:

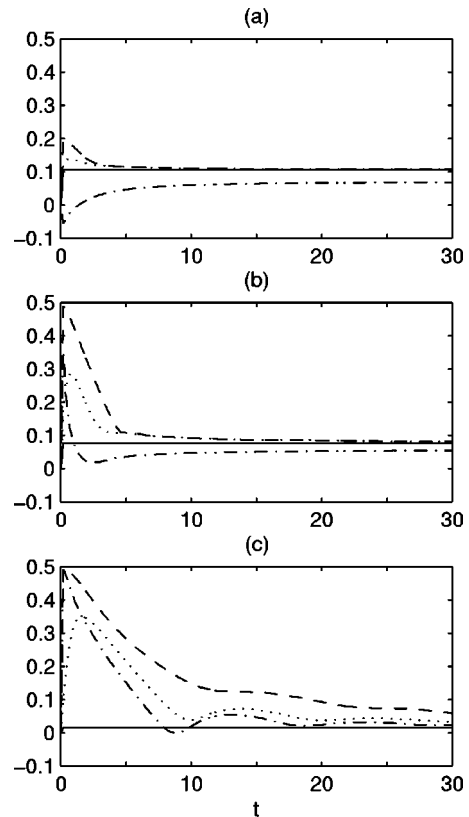


FIG. 3. The growth rates γ_0 (solid line), γ_1 (dashed line), γ_2 (dotted line), γ_3 (dash-dot line), plotted as functions of t for $C=10$ and (a) $\hat{\beta}=10^{-3}$, (b) $\hat{\beta}=1$, and (c) $\hat{\beta}=10$.

$$\xi(t) = \frac{\|\mathbf{u}(t)\|}{\|\mathbf{u}(0)\|}, \quad (17)$$

and its growth rate $\gamma(t) = t^{-1} \ln \xi$. Different choices of initial fluctuation $\mathbf{u}(0)$ produce different energy growth ratios. We consider four energy growth rates $\xi_i(t)$, $i=0, 1, 2, 3$. The first comes from taking $\mathbf{u}(0)$ to be least stable eigenvector of \mathbf{A} , giving

$$\xi_0(t) = e^{\gamma_0 t}, \quad (18)$$

maximum modal growth. The maximum energy growth ratio $\xi_1(t)$ is

$$\xi_1(t) = \max_{\mathbf{u}(0)} \frac{\|\mathbf{u}(t)\|}{\|\mathbf{u}(0)\|} = \|e^{\mathbf{A}t}\|, \quad (19)$$

and does not necessarily correspond to a single initial condition, i.e., the initial condition that produces maximum growth at one instant need not be the same as the initial condition that produces maximum growth at another instant. The quantity $\xi_2(t)$ is defined by using the initial condition that produces maximum growth in the limit of large time. The quantity $\xi_3(t)$ is defined by using the initial condition that produces maximum initial growth. Details regarding the calculation of $\xi_{i=0,1,2,3}(t)$ can be found in the Appendix of Ref. 27.

If \mathbf{A} were normal the growth ratios $\xi_{\{0,1,2,3\}}$ would all coincide. For non-normal operators the statement that applies generally is that $\gamma_0(t)$, $\gamma_1(t)$, and $\gamma_2(t)$ are the same in the

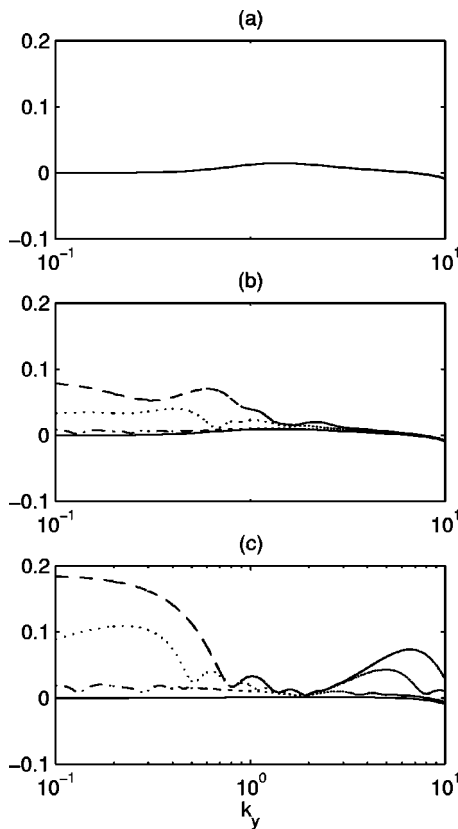


FIG. 4. The growth rates γ_0 (solid line) and $\gamma_1(t)$ for $t=10$ (dashed line), $t=20$ (dotted line), and $t=100$ (dash-dot line) plotted as functions of k_y , for $C=10$ and (a) $\hat{\beta}=10^{-3}$, (b) $\hat{\beta}=1$, and (c) $\hat{\beta}=10$.

limit of large time. Nonmodal growth rates may be larger than the modal growth rate and involve different wave numbers on intermediate time scales. We now examine modal and nonmodal properties of the electromagnetic drift waves in different regimes, considering first the adiabatic regime with $C=10$. Non-normal effects were not observed for the Hasegawa–Wakatani equations in this regime. We now add magnetic fluctuations and consider electrostatic, intermediate, and electromagnetic regimes corresponding, respectively, to $\hat{\beta}=10^{-3}$, $\hat{\beta}=1$, and $\hat{\beta}=10$.

Figures 2 and 3 show the time evolution of the energy growth ratios $\xi_{\{0-3\}}(t)$ and energy growth rates $\gamma_{\{0-3\}}(t)$ for these values of C and $\hat{\beta}$. In the electrostatic regime, nonmodal effects are only important for very small time scales [Figs. 2(a) and 3(a)]. In this regime the maximum growth rate (γ_1) differs from the modal one only on very short time scales, approximately five time units. γ_1 and γ_0 then coincide in the electrostatic regime, as shown in Fig. 2(a). The initial condition that gives maximum growth does not maintain that growth. As $\hat{\beta}$ increases, the nonmodal effects become important on longer time scales. Figures 2(b) and 3(b) show that for the intermediate regime while the modal growth rate γ_0 has decreased, the nonmodal growth rates have increased compared to the electrostatic regime. In the electromagnetic regime this trend continues with the modal growth rate γ_0 approaching zero while the nonmodal growth is enhanced. Also the time scale on which nonmodal behavior is

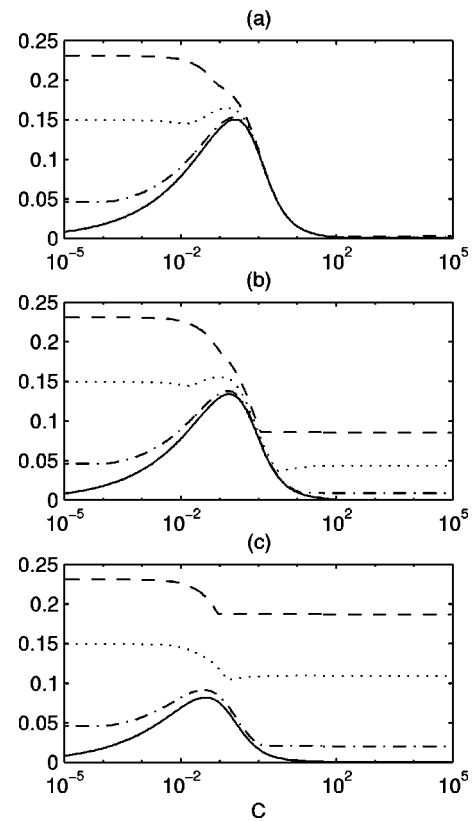


FIG. 5. The growth rates γ_0 (solid line) and $\gamma_1(t)$ for $t=10$ (dashed line), $t=20$ (dotted line), and $t=100$ (dash-dot line) plotted as functions of C , for (a) $\hat{\beta}=10^{-3}$, (b) $\hat{\beta}=1$, and (c) $\hat{\beta}=10$.

important is extended. Although the growth rates $\gamma_1(t)$ and $\gamma_2(t)$ are approaching the modal growth rate γ_0 there continue to be oscillations in the energy ratios.

We now examine which wave numbers are responsible for the modal and nonmodal growth. In Fig. 4, the modal growth rate γ_0 and the maximum growth rate $\gamma_1(t)$ for $t=10, 20, 100$ are shown as functions of k_y for $k_x=0$. The wave number dependence of $\gamma_1(t)$ is different from that of γ_0 for small t . As t increases, the wave number dependence of $\gamma_1(t)$ converges to that of γ_0 . In the electrostatic regime, γ_0 and $\gamma_1(t)$ coincide for all the wave numbers at the times shown. For intermediate to strong magnetic fluctuations, enhanced nonmodal growth is seen over a wide range of wave numbers with the maximum initially occurring at long wavelengths. This growth is larger and takes longer to relax to the modal growth rate as the strength of the magnetic fluctuations is increased. The wave numbers associated with maximum nonmodal growth differ substantially from those associated with modal growth.

We now examine the dependence of the growth rates on the adiabaticity and magnetic fluctuation strength, identifying the regimes where nonmodal behavior is important. Figures 5 and 6 show the dependence of the finite time growth rate $\gamma_1(t)$ and the modal growth rate γ_0 on C and $\hat{\beta}$. Nonmodal growth is important for all values of $\hat{\beta}$ in the hydrodynamics limit of small C , a direct extension of the results obtained for the Hasegawa–Wakatani system.²⁷ However, including moderate to strong magnetic fluctuations leads to

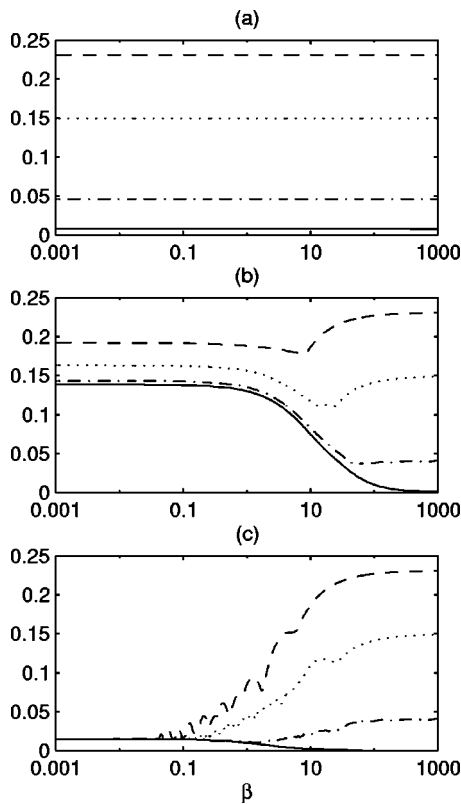


FIG. 6. The growth rates γ_0 (solid line) and $\gamma_1(t)$ for $t=10$ (dashed line), $t=20$ (dotted line), and $t=100$ (dash-dot line) plotted as functions of $\hat{\beta}$, for (a) $C=10^{-5}$, (b) $C=1$, and (c) $C=10$.

significant nonmodal behavior in the adiabatic regime as well. For tokamaks, the estimated values are $C \sim 10$ and $\hat{\beta} \sim 1$, and for these values the linear growth would be much larger than that given by the modal analysis, especially for small times.

Figure 7 shows the wave numbers corresponding to the growth rates in Fig. 5 as a function of C . We denote by k_0^{\max} and $k_1^{\max}(t)$ the perpendicular wave number corresponding to the growth rates γ_0 and $\gamma_1(t)$ ($t=10, t=20$, and $t=100$). In the hydrostatic regime the behavior seen is similar to that observed in the Hasegawa–Wakatani system.²⁷ There is a critical value $C_{\text{crit}}(t)$ of the adiabatic parameter, a decreasing function of time, such that at a particular time t , $k_1^{\max}(t) \approx k_0^{\max}$ for $C < C_{\text{crit}}(t)$ and $k_1^{\max}(t) \approx k_1^{\max}(10)$ for $C > C_{\text{crit}}(t)$. For values of C near the cutoff there is transition connecting the modal and nonmodal behavior. In the adiabatic regime, moderate to strong magnetics fluctuations produce a second regime where nonmodal effects are important. As noted earlier, in Ref. 27 the maximum nonmodal growth is associated with long wavelengths.

V. CONCLUSIONS

We have examined the modal and nonmodal linear behavior of the electromagnetic extension of the Hasegawa–Wakatani model. Nonmodal analysis of the linear behavior of an electromagnetic drift-wave model reveals features not evident from eigenvalue or modal analysis. Nonmodal behavior plays a role in this system because it does not have a

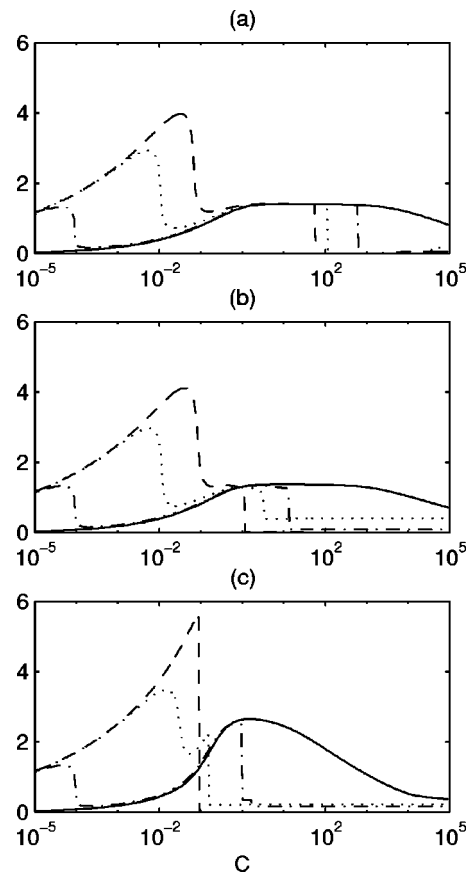


FIG. 7. Values of k_0^{\max} (solid line) and $k_1^{\max}(t)$ for $t=10$ (dashed line), $t=20$ (dotted line), and $t=100$ (dash-dot line) plotted as functions of C , for (a) $\hat{\beta}=10^{-3}$, (b) $\hat{\beta}=1$, and (c) $\hat{\beta}=10$.

complete set of orthogonal eigenvectors. Two parameters determine the importance of the nonmodal effects, the adiabaticity parameter C and the electromagnetic parameter $\hat{\beta}$. Examination of the pseudospectrum shows that while the modal growth rate goes to zero in the hydrodynamic limit, nonmodal growth is still present. Calculation of the numerical abscissa showed that in the adiabatic regime the instantaneous rate of the change of the energy can be many orders of magnitude larger than the modal growth rate.

In the hydrodynamic regime (small values of C), the linear properties are practically independent of $\hat{\beta}$ and the modal growth rate gives only poor estimates of the general nonmodal behavior. In the adiabatic regime, on the other hand, the nonmodal behavior is important only for large values of $\hat{\beta}$ (electromagnetic limit) and the maximum instantaneous growth rate is much larger than the modal growth rate.

These conclusions suggest that when studying the full nonlinear simulations of this electromagnetic system and comparing with the linear properties, it is important to consider the non-normal character of the system. As non-normality appears to be generic for multiple-fields models of plasma fluctuations,²⁰ this line of study is important to pursue the understanding of transition to turbulence and submarginal turbulence in plasmas.

ACKNOWLEDGMENTS

This work was supported by FAPESP (Fundação de Amparo à Pesquisa do Estado de São Paulo) under Grant No. 96/5388-0 and by CNPq (Conselho Nacional de Desenvolvimento Científico e Tecnológico) under Grant Nos. 381737/97-73 and 520945/94-8.

- ¹F. L. Hinton and R. D. Hazeltine, *Rev. Mod. Phys.* **48**, 239 (1976).
- ²A. J. Wootton, B. A. Carreras, H. Matsumoto, K. McGuire, W. A. Peebles, Ch. P. Ritz, P. W. Terry, and S. J. Zweben, *Phys. Fluids B* **2**, 2879 (1990).
- ³W. Horton, *Phys. Rep.* **192**, 1 (1990).
- ⁴S. Raychardhuri, *Nucl. Fusion* **35**, 1281 (1995).
- ⁵The ASDEX Team, *Nucl. Fusion* **29**, 1959 (1989).
- ⁶F. Wagner, G. Becker, K. Behringer, D. Campbell, A. Eberhagen, W. Engelhardt, G. Fussmann, O. Gehre, J. Gernhardt, G. V. Gierke, G. Haas, M. Huang, F. Karger, M. Keilhacker, O. Klueber, M. Kornherr, K. Lackner, G. Lisitano, G. G. Lister, H. M. Mayer, D. Meisel, E. R. Mueller, H. Murmann, H. Niedermeyer, W. Poschenrieder, H. Rapp, H. Roehr, F. Schneider, G. Siller, E. Speth, A. Staebler, K. H. Steuer, G. Venus, O. Vollner, and Z. Yue, *Phys. Rev. Lett.* **49**, 1408 (1982).
- ⁷R. J. Groebner, *Phys. Fluids B* **5**, 2343 (1993).
- ⁸R. D. Durst, R. J. Fonck, J. S. Kim, S. F. Paul, N. Bretz, C. Bush, Z. Chang, and R. Hulse, *Phys. Rev. Lett.* **71**, 3135 (1993).
- ⁹N. Mattor and P. H. Diamond, *Phys. Plasmas* **1**, 4002 (1994); N. Mattor, *ibid.* **2**, 766 (1995).
- ¹⁰B. Scott, *Plasma Phys. Controlled Fusion* **39**, 1635 (1997).
- ¹¹B. Rogers and J. F. Drake, *Phys. Rev. Lett.* **79**, 229 (1997).
- ¹²A. Zeiler, D. Biskamp, J. F. Drake, and P. N. Guzdar, *Phys. Plasmas* **3**, 2951 (1996).
- ¹³O. Pogutse and Yu. Igitkhanov, *Proceedings of the Edge-Plasma Theory and Simulation Workshop, Innsbruck, Austria, 1998*, [*Czech. J. Phys.* **48/S2**, 39 (1998)].
- ¹⁴S. J. Camargo, B. D. Scott, and D. Biskamp, *Phys. Plasmas* **3**, 3912 (1996).
- ¹⁵L. N. Trefethen, A. E. Trefethen, S. C. Reddy, and T. A. Driscoll, *Science* **261**, 578 (1993).
- ¹⁶K. M. Butler and B. F. Farrell, *Phys. Fluids A* **4**, 1637 (1992).
- ¹⁷J. S. Baggett, T. A. Driscoll, and L. N. Trefethen, *Phys. Fluids* **7**, 833 (1995).
- ¹⁸F. Waleffe, *Phys. Fluids* **7**, 3060 (1995).
- ¹⁹F. Waleffe, *Phys. Fluids* **9**, 883 (1997).
- ²⁰J. A. Krommes, *Proceedings of the 1998 International Congress on Plasma Physics combined with the 25th European Physical Society Conference on Controlled Fusion and Plasma Physics, Prague, Czech Republic, 1998* [*Plasma Phys. Controlled Fusion* **41/S3**, A641 (1999)].
- ²¹A. Hasegawa and M. Wakatani, *Phys. Rev. Lett.* **50**, 682 (1985).
- ²²J. F. Drake, A. Zeiler, and D. Biskamp, *Phys. Rev. Lett.* **75**, 4222 (1995).
- ²³S. J. Camargo, M. K. Tippet, and I. L. Caldas, *Proceedings of the Edge-Plasma Theory and Simulation Workshop, Innsbruck, Austria, 1998* [*Czech. J. Phys.* **48/S2**, 189 (1998)].
- ²⁴M. K. Tippet, S. J. Camargo, and I. L. Caldas, *Topics in Theoretical Physics*, Festschrift for Abraham H. Zimerman, Vol. II, edited by H. Aratyn, L. A. Ferreira, and J. F. Gomes (Instituto de Física Teórica, São Paulo, Brazil, 1998), p. 47.
- ²⁵A. Hasegawa and M. Wakatani, *Phys. Fluids* **26**, 2770 (1983).
- ²⁶R. D. Hazeltine, *Phys. Fluids* **26**, 3242 (1983).
- ²⁷S. J. Camargo, M. K. Tippet, and I. L. Caldas, *Phys. Rev. E* **58**, 3693 (1998).
- ²⁸N. Bekki and Y. Kaneda, *Phys. Rev. Lett.* **57**, 2176 (1986).
- ²⁹J. F. Drake, T. M. Antonsen, Jr., A. B. Hassam, and N. T. Glad, *Phys. Fluids* **26**, 2509 (1983).
- ³⁰B. D. Scott and A. B. Hassam, *Phys. Fluids* **30**, 90 (1987).
- ³¹S. J. Camargo, D. Biskamp, and B. D. Scott, *Phys. Plasmas* **2**, 48 (1995).
- ³²D. Biskamp, *Nonlinear Magnetohydrodynamics* (Cambridge University Press, Cambridge, 1993), p. 17.
- ³³D. Biskamp, S. J. Camargo, and B. D. Scott, *Phys. Lett. A* **186**, 239 (1994).
- ³⁴L. N. Trefethen, *SIAM Rev.* **39**, 383 (1997).